FOS WAVELENGTH SCALE BELOW THE CALIBRATION LAMP CUTOFF AT 1239Å (Laboratory Calibration Plan 13B)

M. SIRK and R. BOHLIN
SPACE TELESCOPE SCIENCE INSTITUTE

Instrument Science Report CAL/FOS—038
October 1986

Abstract

Since the FOS internal Pt–Cr–Ne calibration lamps have no useful emission lines below 1239Å, the standard wavelength calibration at the shortest wavelengths around 1150Å is uncertain by about 10 times the typical error at longer wavelengths. A new technique is developed to extend the calibrations down to the blue Digicon cutoff at 1150Å for gratings G130H and G160L. Estimated uncertainties at 1150Å are 0.14Å (37 km s^{-1}) for G130H and 1.0Å (260 km s^{-1}) for G160L, while the corresponding uncertainties at Lα (1216Å) are 0.068Å (17 km s^{-1}) and 0.8Å (200 km s^{-1}), respectively. This is an improvement of up to a factor of 2 for G130H and up to a factor of 5 for G160L. However, the above errors at 1150Å are still worse than the typical RMS error found at longer wavelengths by about a factor of 5. At Lα the uncertainty is only about 3 times the RMS scatter at the longer wavelengths.

Features on the G160L calibration spectrum have been assigned new vacuum wavelengths by determining line centers of features on high resolution FOS spectra that are smoothed to the G160L resolution.

I. Introduction

Due to the lack of reference lines in the far UV, the previous wavelength calibrations (Sirk and Bohlin 1986a) of the high dispersion grating G130H ($\approx$ 1Å/diode) and the low dispersion grating G160L ($\approx$ 7Å/diode) have estimated errors of 0.28 and 5Å, respectively, at the 1150Å cutoff. These errors are over an order of magnitude greater than the RMS error in the regions where there are reference lines, and thus, indicate the need for a better method of calibrating G130H and G160L in the far UV. In addition, due to the low dispersion of G160L, virtually all the features seen on the calibration spectra are blends of several lines, complicating the assignment of correct wavelengths to these features.

This report outlines a method for extending the calibrations for both G130H and G160L with error estimates down to the 1150Å cutoff, and for improving the calibration of G160L over its entire range.

II. Methodology

All internal spectra utilized in this report were taken with the direct calibration lamp, not the cross-strapped lamp. Two data sets are used from the July, 1984 Thermal Vacuum Calibrations at Martin Marrietta Corp. that were obtained with photocathode temperatures of -10 C ("hot") and -30 C ("cold"). On the blue tube in the region from diode 0 to 250, wavelength as a function of diode number is linear within the errors of measurement for four FOS gratings, as can be seen in Figure 1. Since the dispersion appears linear, a linear fit to the found line positions on G130H and G160L can be extrapolated down to the 1150Å cutoff to provide good estimates for wavelength scales in the far UV.

Linear fits are performed to determine wavelength as a function of diode number for the eight shortest wavelength lines in the G130H spectra. Residuals for the four cases (upper and lower aperture, cold and hot data sets) are shown as Figure 2. No evidence for systematic curvature is seen. Rather than having two sets of dispersion coefficients for G130H (*i.e.* linear for the far UV, and cubic for the remainder of the grating), artificial pixel values are estimated for selected far UV wavelengths from the linear coefficients and appended as data points for the least squares cubic solution for the dispersion constants on G130H. The lower 0.1–Pair aperture, cold data set is chosen to be consistent with the calibrations in Sirk and Bohlin (1986a). The result is one set of cubic coefficients that provide an accurate wavelength scale for the entire range of the grating. The residuals of the cubic fit to the data that include three artificial points are shown in Figure 3. Table 1 lists the vacuum wavelength, pixel position, and residuals, including the three artificial data points, for G130H. The spectrum is YAU0011; and the line centroids are found according to the technique of Sirk and Bohlin (1986a). The number of artificial data points is chosen to match the mean density of real lines in the spectrum. With the addition of the three artificial data points, the RMS error increased from 0.019 to 0.024 diode and the range of calibrated coverage increased by 20%.

Once an accurate dispersion relation for G130H was obtained, calibration spectra from G130H, G190H, and G270H were smoothed to the resolution of G160L. For all features that satisfied the line selection criteria outlined in section III of Sirk and Bohlin 1986a, effective

wavelengths are found by determining the centers of the smoothed features from the high dispersion gratings. Figure 4 shows the smoothed spectra from G130H, G190H, and G270H, and Figure 5 shows the calibration spectrum for G160L. The indicated vacuum wavelengths are determined from the smoothed high resolution spectra. Table 2 lists the new vacuum wavelengths, the old vacuum wavelengths, the pixel position, and the residuals from a cubic fit for the lower 0.1–Pair aperture, cold data set, spectrum YAU0016. In the same manner as G130H, a linear fit is performed on the eleven shortest wavelength lines of G160L, the residuals of which are shown as Figure 6. Pixel values are estimated for four far UV wavelengths from the linear coefficients and then appended as data points for the G160L solution. A cubic fit is performed and yields a wavelength scale for the entire range of the grating. The cubic residuals are plotted in Figure 7. The RMS error, including the four artificial points, is reduced from 0.061 diodes from the previous calibration (Table 3, Sirk and Bohlin 1986a) to 0.039 diodes.

Uncertainties in the wavelength scales in the far UV are dominated by the uncertainties in the predicted pixel positions that were estimated by extrapolating the linear fit to G130H and the linear fit to G160L. To estimate these uncertainties for G130H, the difference is found between predicted position from the linear fit to the eight shortest wavelength lines and a linear fit to the five shortest wavelength lines. On G160H the differences are found between the linear fit to the eleven and seven shortest wavelength lines. These differences, calculated at 1150 and 1216Å, for the upper and lower aperture spectra for the hot and cold data sets are listed in Table 3 for both gratings. The upper aperture, hot data set is the worst case for both dispersers. The uncertainties in the wavelength scales at 1150 and 1216Å are calculated by adding in quadrature the RMS error of the cubic fit to the worst case errors of Table 3. For G130H the errors are 0.14Å (37 km s^{-1}) and 0.068Å (17 km s^{-1}) and for G160L 1.0Å (260 km s^{-1}) and 0.8Å (200 km s^{-1}) at 1150 and 1216Å, respectively. The RMS errors in the regions where the cubic fits are constrained by actual emission lines (longward of 1238Å for G130H and longward of 1524Å for G160L) are 0.024Å (5.5 km s^{-1}) for G130H and 0.27Å (51 km s^{-1}) for G160L.

The new extended calibrations of G130H and G160L are compared to the old ones of Table 3 in Sirk and Bohlin (1986a) by determining the difference in predicted wavelength as a function of diode number and are shown as Figures 8 and 9, respectively. In the region

of actual emission lines, the wavelength scales agree to within the RMS errors of the cubic fits. In the regions where pixel values were estimated, the wavelength scales are divergent indicating that cubic fits should not be used to extrapolate wavelength scales.

An external Pt–Cr–Ne spectrum is investigated as an independent check of the validity of the calibration procedure outlined above for G130H. The external lamp spectrum shows proportionately much more flux in the far UV than the internal lamps (Sirk and Bohlin 1985). Five more identifiable lines are found in the external lamp spectrum between 1170 and 1238Å. The differences in position of features between the internal and external lamp spectra are non–linear as shown for G130H in Figure 10. A straight line fit is performed in the region between 1239Å (diode 148) and 1410Å (diode 318) to determine internal pixel position as a function of external pixel position for the found line centers. The estimated error of this linear extrapolation to 1150Å (diode 60) of the steeply sloped regions of Figure 10 is uncertain to 0.15Å for both the hot and cold cases. The found pixel positions of the five shortest wavelength lines of the external spectrum are adjusted to the system of the internal spectrum by extrapolating the linear fit out to 1170Å (diode 80). The difference between the cubic fits of the two methods of extending the calibration of G130H down to the 1150Å cutoff (*i.e.* a. extrapolating a linear fit of an internal spectrum or b. appending five additional lines from an external spectrum to an internal one) is 0.06Å at the 1150Å cutoff, well within the 0.15Å uncertainty estimated for both of the methods at this wavelength.

III. Applicability to the Flight Data Reduction

Since the artificial wavelengths and their corresponding pixel values in the first sections of Tables 1 and 2 do not correspond to features that can be found on calibration spectra, they are not added to the line libraries of G130H and G160L. Thus, in order to accurately calibrate template spectra obtained with these gratings, the entire scenario outlined in this report should be repeated for G130H and G160L. See Sirk and Bohlin (1986c) for the definition and use of template spectra. For G160L, the determination of wavelengths from smoothed high resolution spectra would not be essential. However, the verification of all results in this report with flight data will add confidence in the validity of the pipeline calibration process.

A summary of the post–launch calibration procedure required to reduce a G130H template spectrum follows:

1) Fit the found lines below 1450Å (≈ pixel 325) with a straight line.

2) Use the coefficients of the straight line fit to predict pixel positions at 1150, 1180, and 1210Å.

3) Do a cubic fit to the actual found pixel positions combined with the artificial line positions from Step 2.

For G160L, the procedure is analogous: the wavelength limit is 1950Å (≈ pixel 30) for Step 1 and the wavelengths for Step 2 are 1150, 1207.5, 1265, and 1322.5Å. In addition, the line library derived from lab data for G160L features should be repeated after launch using the high dispersion template spectra.

References

Sirk, M., and Bohlin, R. 1985, *Internal FOS Pt-Cr-Ne Calibration Lamps, Performance in the Far UV* CAL/FOS-014, March 22, STScI.

Sirk, M., and Bohlin, R. 1986a, *FOS Wavelength Calibration* CAL/FOS-026, February, STScI.

Sirk, M., and Bohlin, R. 1986b, *FOS Entrance Aperture Offsets* CAL/FOS-029, May, STScI.

Sirk, M., and Bohlin, R. 1986c, *FOS Wavelength Calibration Exposure Times* CAL/FOS-028, April, STScI.

TABLE 1.

Vacuum wavelengths, pixel values, and residuals for G130H

VACUUM	PIXEL[b]	RESIDUAL
1150.000a	59.961	-0.030
1180.000a	89.746	0.012
1210.000a	119.531	0.027
1238.852	148.195	0.004
1248.610	157.831	0.051
1271.793	180.917	-0.032
1309.496c	218.313	-0.019
1327.432	236.093	0.000
1378.956	287.269	-0.015
1382.046	290.359	-0.035
1410.135	318.239	0.009
1482.826	390.657	0.010
1494.726	402.540	0.010
1509.272c	417.085	0.003
1524.704	432.511	0.016
1530.199c	438.006	0.024
1534.894c	442.734	-0.001
1554.929	462.829	-0.009
1574.322c	482.297	-0.001
1581.399	489.434	-0.023
	RMS =	0.024

a These three "lines" are not visible on G130H spectra but have estimated pixel values as explained in the text.

b Pixel values are from the internal G130H spectrum YAU0011, lower aperture taken at -30 C.

c Two component blend.

TABLE 2.
Wavelength Library For Grating G160L
Estimated From High Resolution Gratings.

NEW VACUUM	OLD VACUUM	PIXELb	RESIDUAL
1150.000a		318.542	-0.043
1207.500a		326.778	-0.019
1265.000a		335.013	-0.001
1322.500a		343.249	0.009
1379.429		351.469	-0.052
1404.257		354.910	0.065
1432.374		358.983	0.020
1525.002	1524.704	372.265	0.004
1555.191		376.542	0.049
1574.635		379.364	0.011
1635.002		387.965	0.052
1723.381		400.720	-0.049
1776.986	1776.920	408.367	-0.019
1883.407	1883.079	423.594	0.004
1915.936	1916.083	428.228	0.035
2050.477	2050.097	447.606	-0.030
2085.948	2085.969	452.665	0.009
2129.504	2129.283	458.985	-0.046
2144.925	2144.922	461.173	-0.014
2175.425	2175.352	465.570	-0.019
2202.693	2202.806	469.486	-0.006
2246.339		475.786	-0.012
2263.651	2263.363	478.313	-0.040
2275.090	2275.083	479.947	-0.023
2291.816		482.253	0.086
2440.452	2440.797	503.824	0.033
2468.264	2468.688	507.899	-0.005
2488.043	2487.919	510.761	0.006
			RMS = 0.039

a These first four "lines" are not visible on G160L spectra but have estimated pixel values as explained in the text.

b Pixel values are from the internal G160L spectrum YAU0016, lower aperture, taken at -30 C.

Table 3

Differences in Diodes between Different Linear Fits

	G130H			
	Lower Aperture		Upper Aperture	
	1150Å	1216Å	1150Å	1216Å
Cold	-.028	-.013	-.062	-.028
Hot	-.071	-.032	-.14	-.064
	G160L			
Cold	-.059	-.046	-.11	-.082
Hot	-.086	-.067	-.14	-.11

Figure Captions

Figure 1. Residuals from linear fits of wavelength as a function of diode number over a restricted range for four FOS gratings on the blue detector. There is no evidence of systematic curvature in any of the four plots.

Figure 2. Residuals from a linear fit over a restricted wavelength range on G130H for four different cases (upper and lower apertures, hot and cold data sets). UH, UC, LH, and LC refer to the upper hot, upper cold, lower hot and lower cold data sets, respectively. The lowest plot is the same as the lowest plot in Figure 1. As for Figure 1, there is no evidence of systematic curvature.

Figure 3. Residuals from a cubic fit for G130H including the three points (denoted *) that were estimated from the linear fit of Figure 2.

Figure 4. Internal wavelength calibration spectra from G130H, G190H, and G270H smoothed to the resolution of G160L. Arrows indicate the boundries of the three gratings.

Figure 5. The internal G160L spectrum used for the calibration. Features are labeled with their vacuum wavelengths that were determined from the smoothed high resolution spectra of Figure 4.

Figure 6. Linear residuals from the 11 shortest wavelength lines visible on G160L.

Figure 7. Cubic residuals from G160L including the four points (denoted *) that were estimated from the linear fit of Figure 6.

Figure 8. Differences in Ångstroms between the old cubic and new cubic fits for the lower aperture cold spectrum on G130H. The fits are divergent in the region shortward of diode 150 where there are no reference lines. From diode 150 to 516 the fits agree within their RMS errors.

Figure 9. Differences in Ångstroms between the old cubic and new cubic fits for the lower aperture cold spectrum on G160L. The fits are divergent in the region shortward of diode 340 where there are no reference lines. From diode 340 to 516 the fits agree within their RMS errors.

Figure 10. Differences in found pixel position between the external and internal Pt–Cr–Ne calibration lamp lower aperture spectra for the cold and hot data sets, denoted + and □, respectively. The two depicted cases are from the July, 1984 Thermal Vacuum Calibrations at Martin Marrietta Corp. obtained with photocathode temperatures of -10 C ("hot") and -30 C ("cold"). The hot data has a constant of 0.2 diode added for plotting purposes.

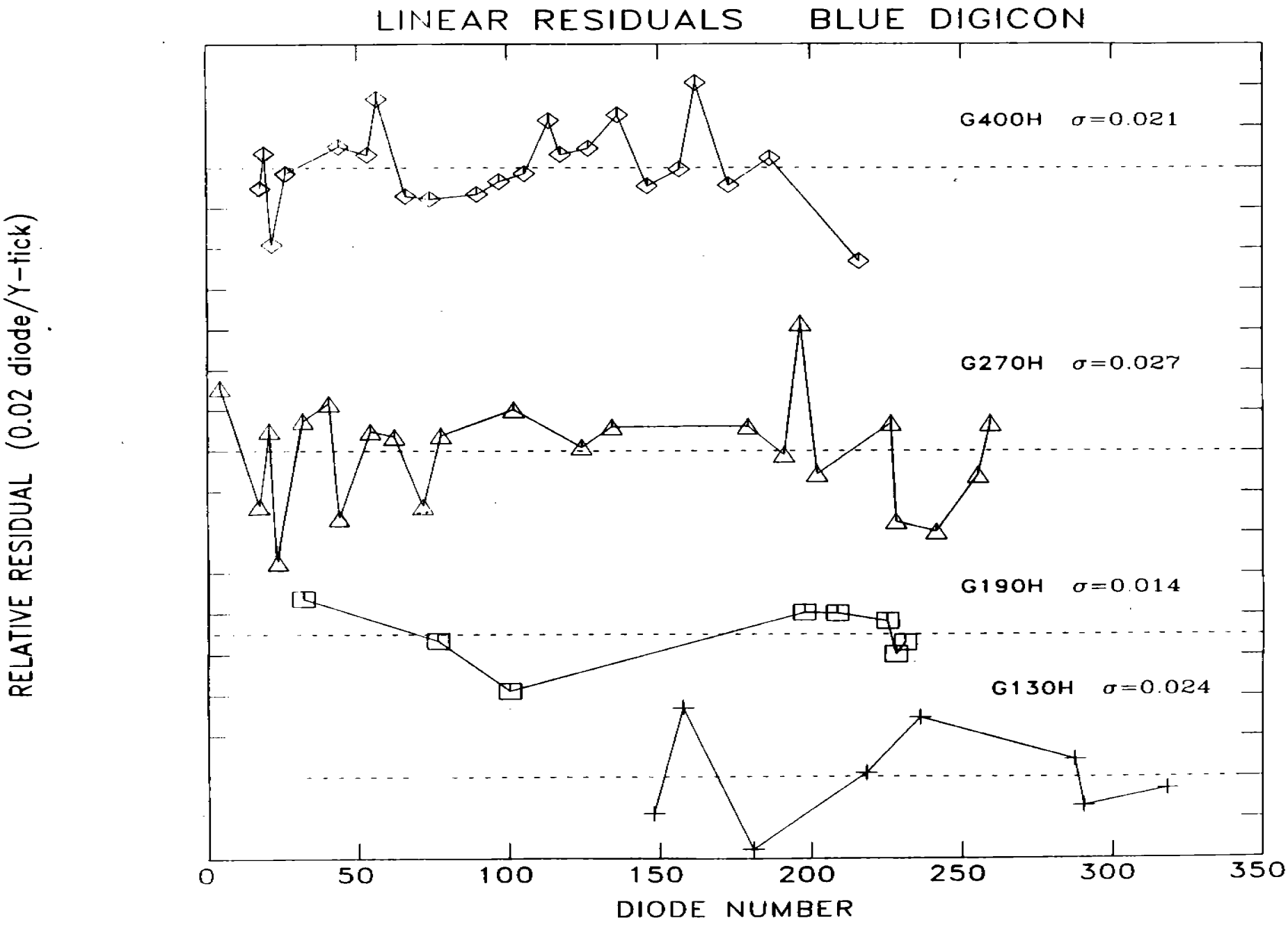
LINEAR RESIDUALS BLUE DIGICON
G400H σ=0.021
G270H σ=0.027
G190H σ=0.014
G130H σ=0.024
RELATIVE RESIDUAL (0.02 diode/Y-tick)
0
50
100
150
200
250
300
350
DIODE NUMBER

Figure 1.

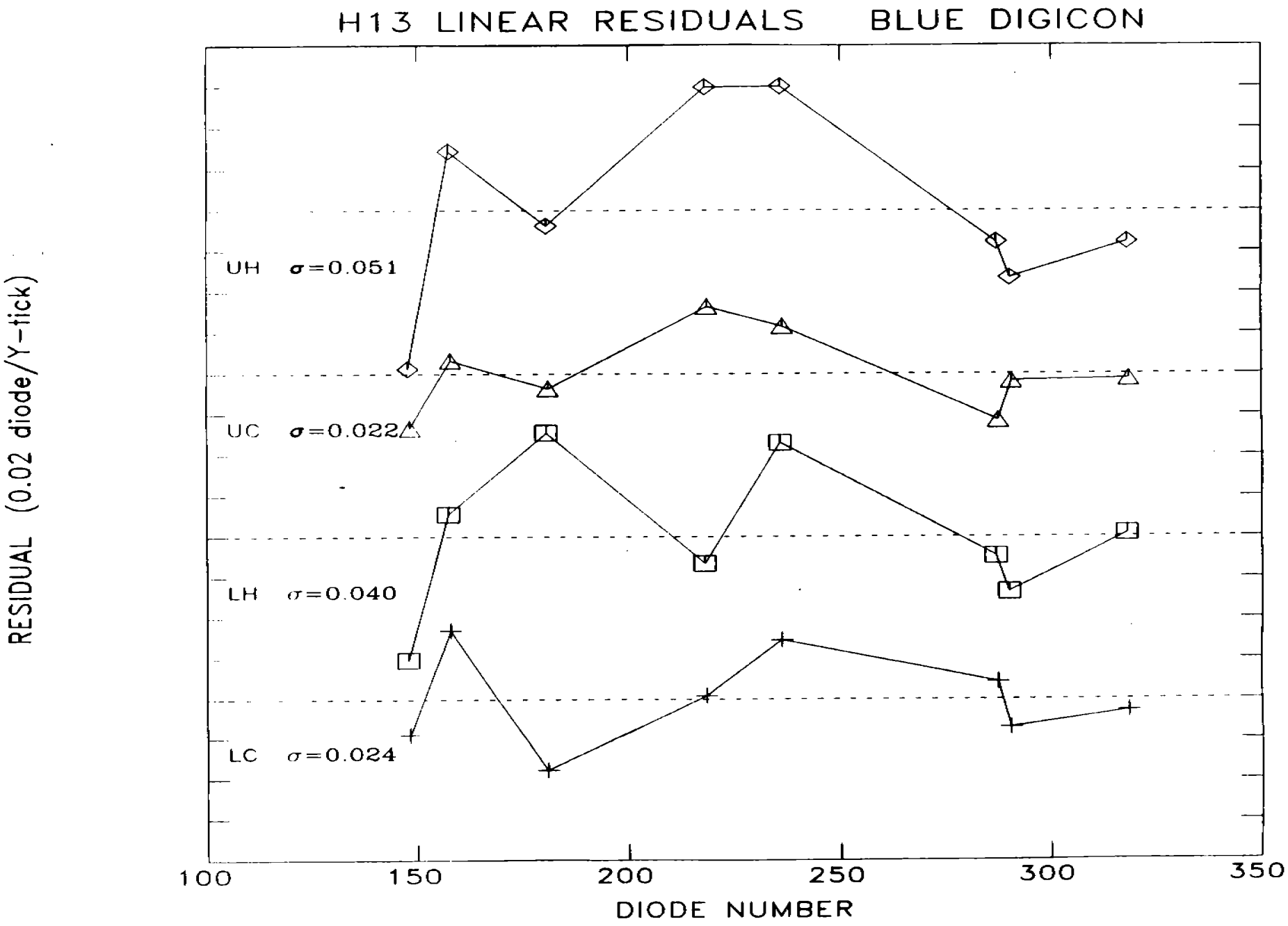
H13 LINEAR RESIDUALS BLUE DIGICON
RESIDUAL (0.02 diode/Y-tick)
UH σ=0.051
UC σ=0.022
LH σ=0.040
LC σ=0.024
100
150
200
250
300
350
DIODE NUMBER

Figure 2.

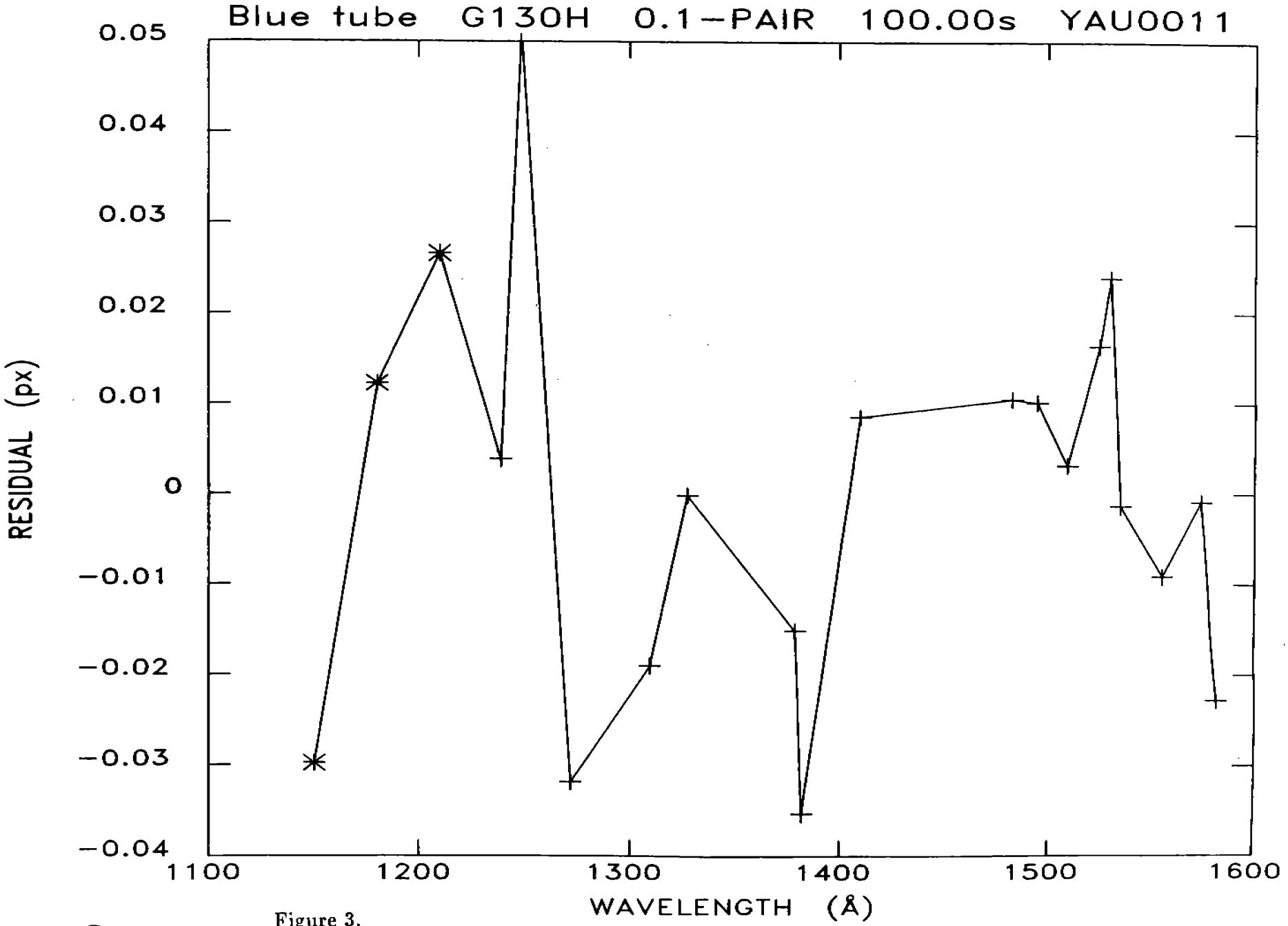
Blue tube G130H 0.1−PAIR 100.00s YAU0011
RESIDUAL (px)
0.05
0.04
0.03
0.02
0.01
0
−0.01
−0.02
−0.03
−0.04
1100
1200
1300
1400
1500
1600
WAVELENGTH (Å)

Figure 3.

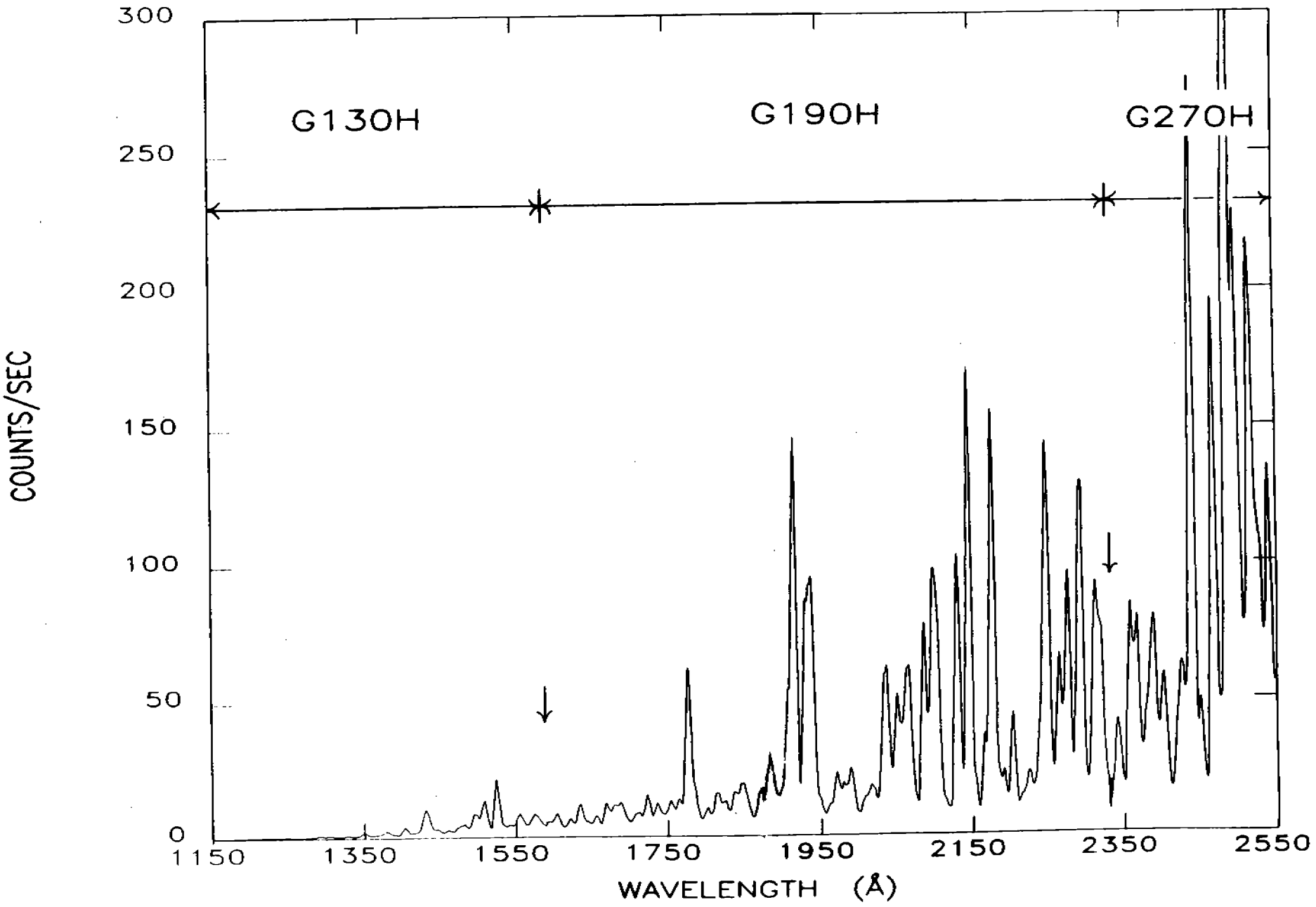
G130H
G190H
G270H
300
250
200
150
100
50
0
COUNTS/SEC
1150
1350
1550
1750
1950
2150
2350
2550
WAVELENGTH (Å)

Figure 4.

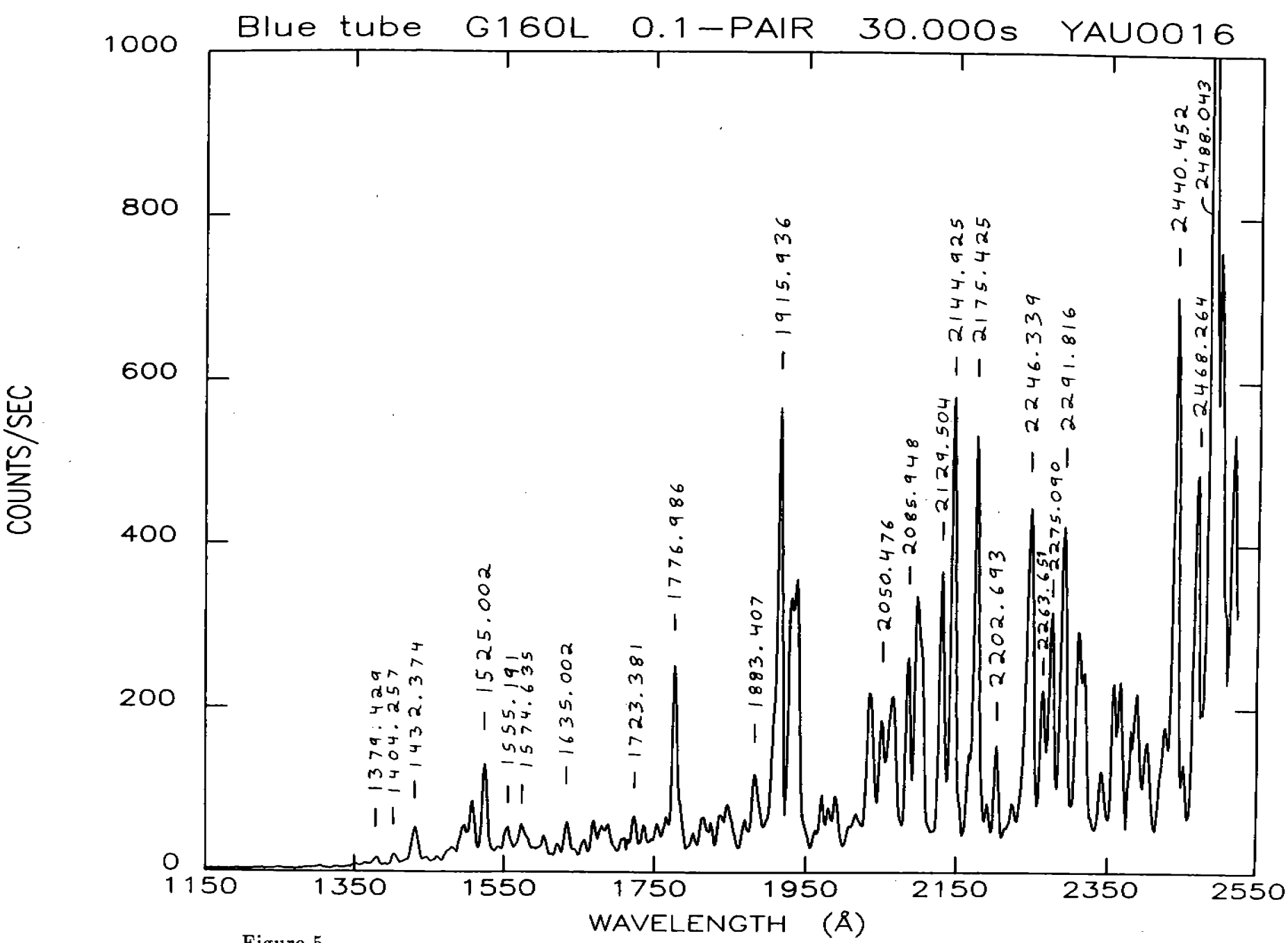
Blue tube G160L 0.1—PAIR 30.000s YAU0016
COUNTS/SEC
WAVELENGTH (Å)
1000
800
600
400
200
0
1150
1350
1550
1750
1950
2150
2350
2550
1379.429
1404.257
1432.374
1525.002
1555.191
1574.635
1635.002
1723.381
1776.986
1893.407
1915.936
2050.476
2085.948
2129.504
2144.925
2175.425
2202.693
2246.339
2263.651
2275.090
2291.816
2440.452
2468.264
2488.043

Figure 5.

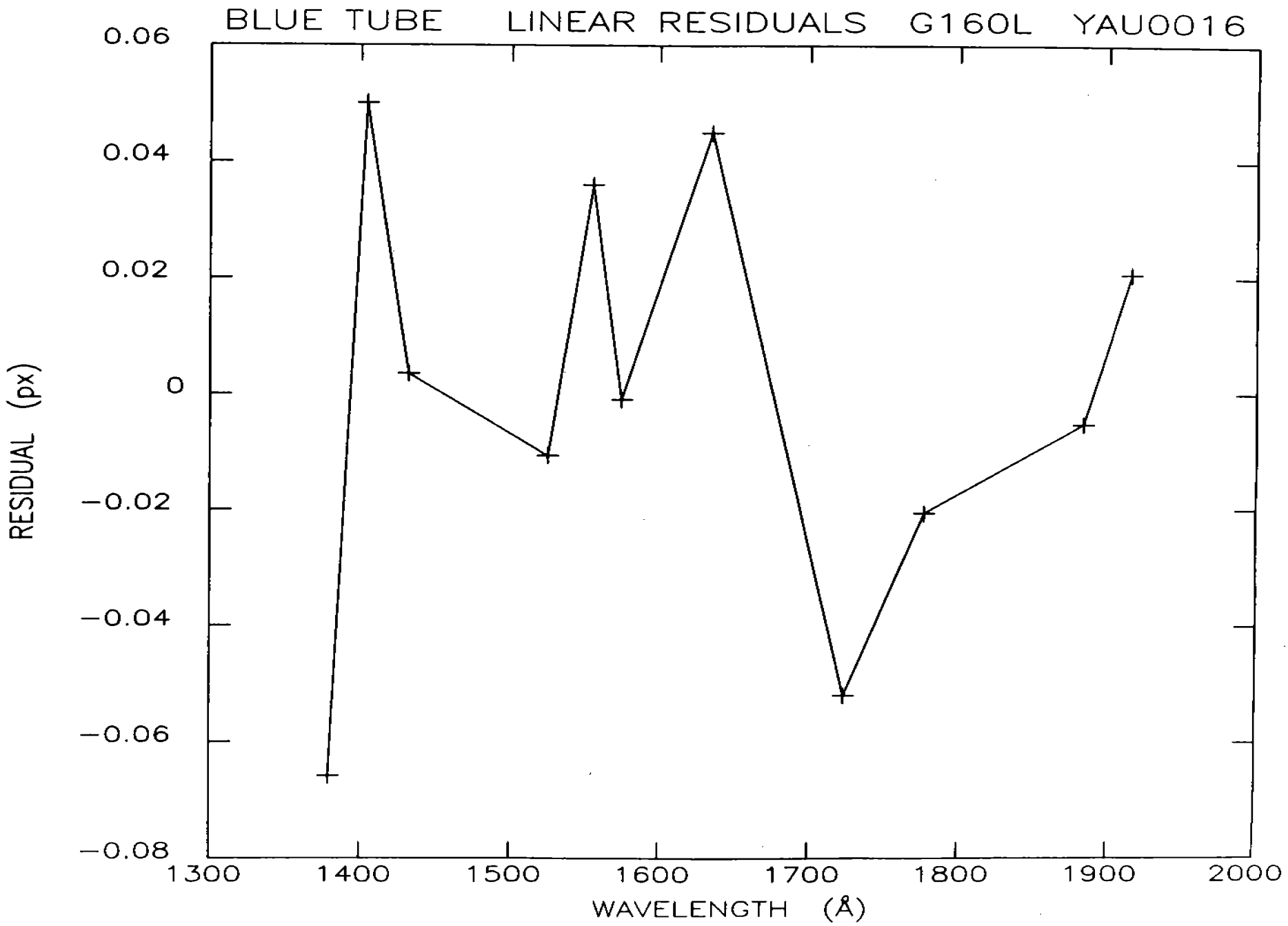
BLUE TUBE LINEAR RESIDUALS G160L YAU0016
0.06
0.04
0.02
0
−0.02
−0.04
−0.06
−0.08
RESIDUAL (px)
1300
1400
1500
1600
1700
1800
1900
2000
WAVELENGTH (Å)

Figure 6.

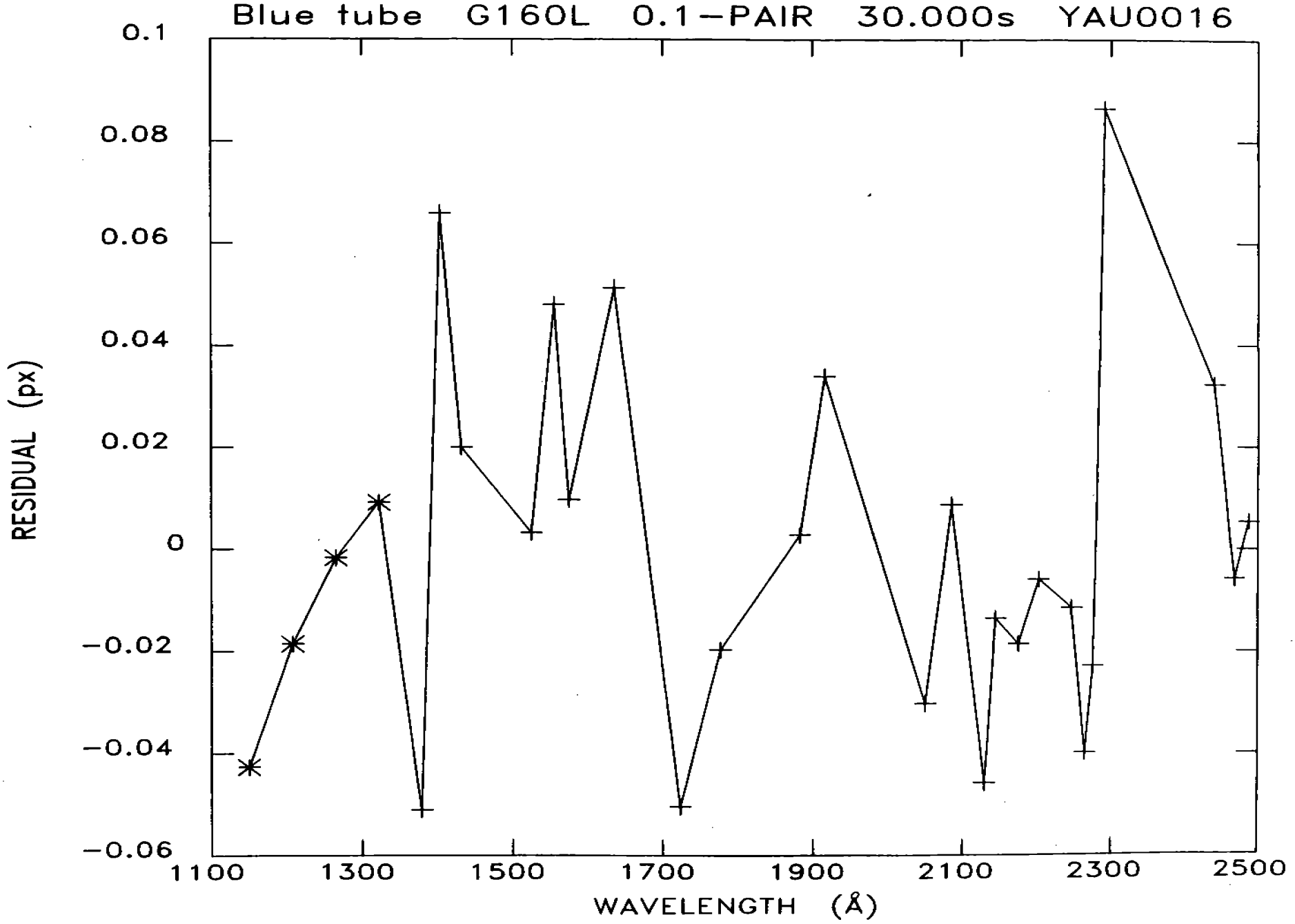
Blue tube G160L 0.1−PAIR 30.000s YAU0016
RESIDUAL (px)
0.1
0.08
0.06
0.04
0.02
0
−0.02
−0.04
−0.06
1100
1300
1500
1700
1900
2100
2300
2500
WAVELENGTH (Å)

Figure 7.

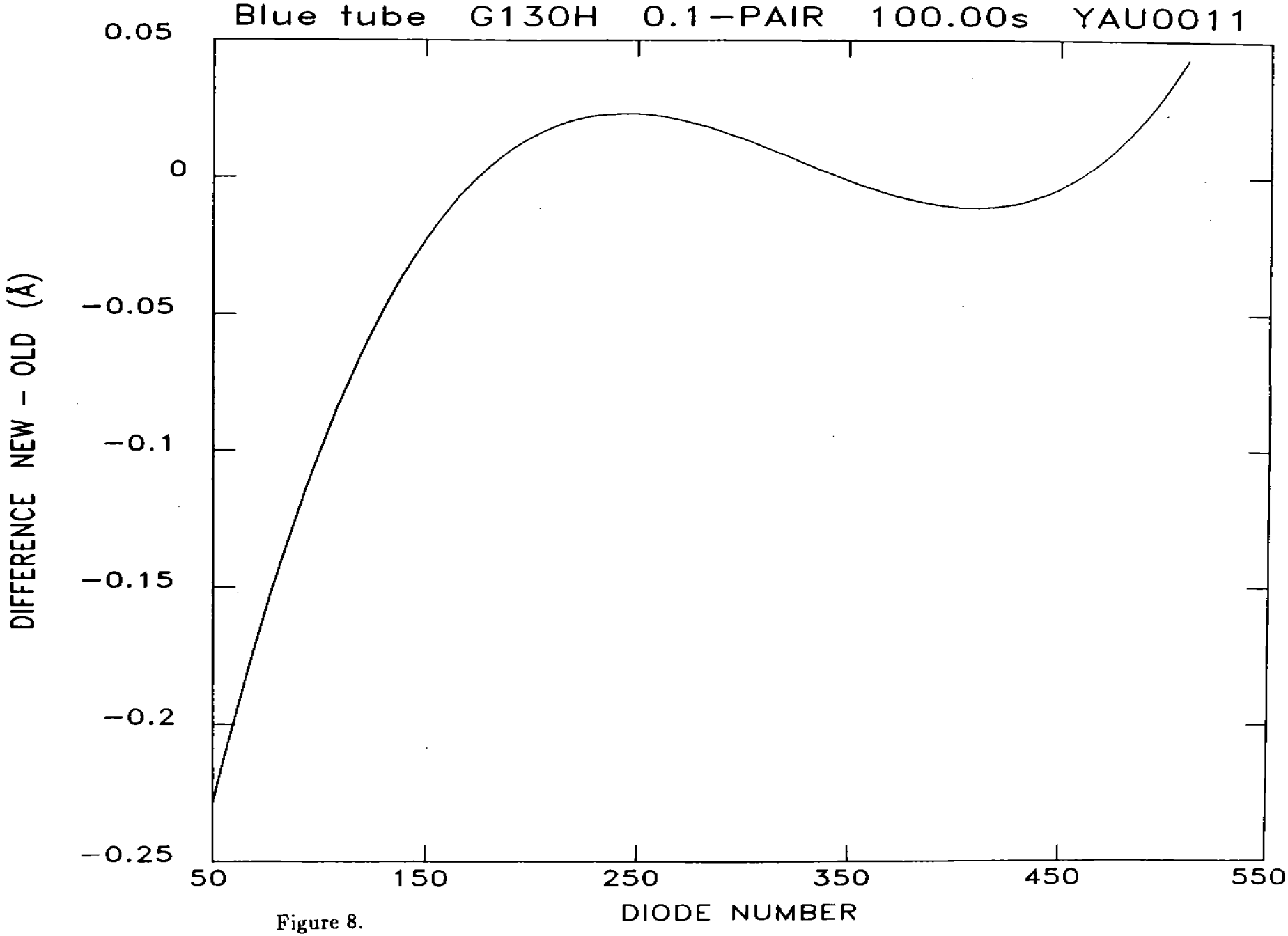
Blue tube G130H 0.1–PAIR 100.00s YAU0011
0.05
0
−0.05
−0.1
−0.15
−0.2
−0.25
DIFFERENCE NEW – OLD (Å)
50
150
250
350
450
550
DIODE NUMBER

Figure 8.

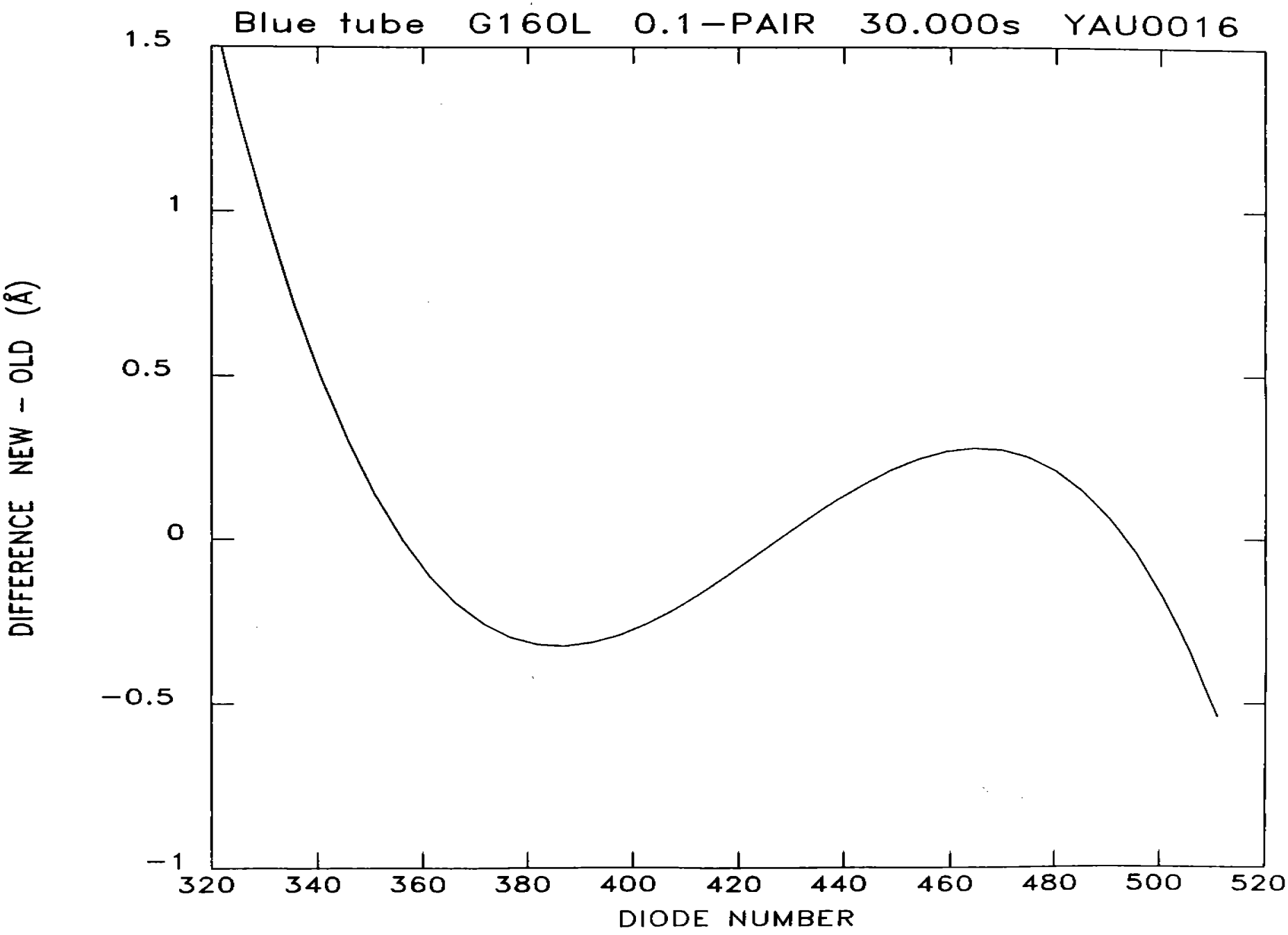
Blue tube G160L 0.1—PAIR 30.000s YAU0016
1.5
1
0.5
0
−0.5
−1
DIFFERENCE NEW - OLD (Å)
320
340
360
380
400
420
440
460
480
500
520
DIODE NUMBER

Figure 9.

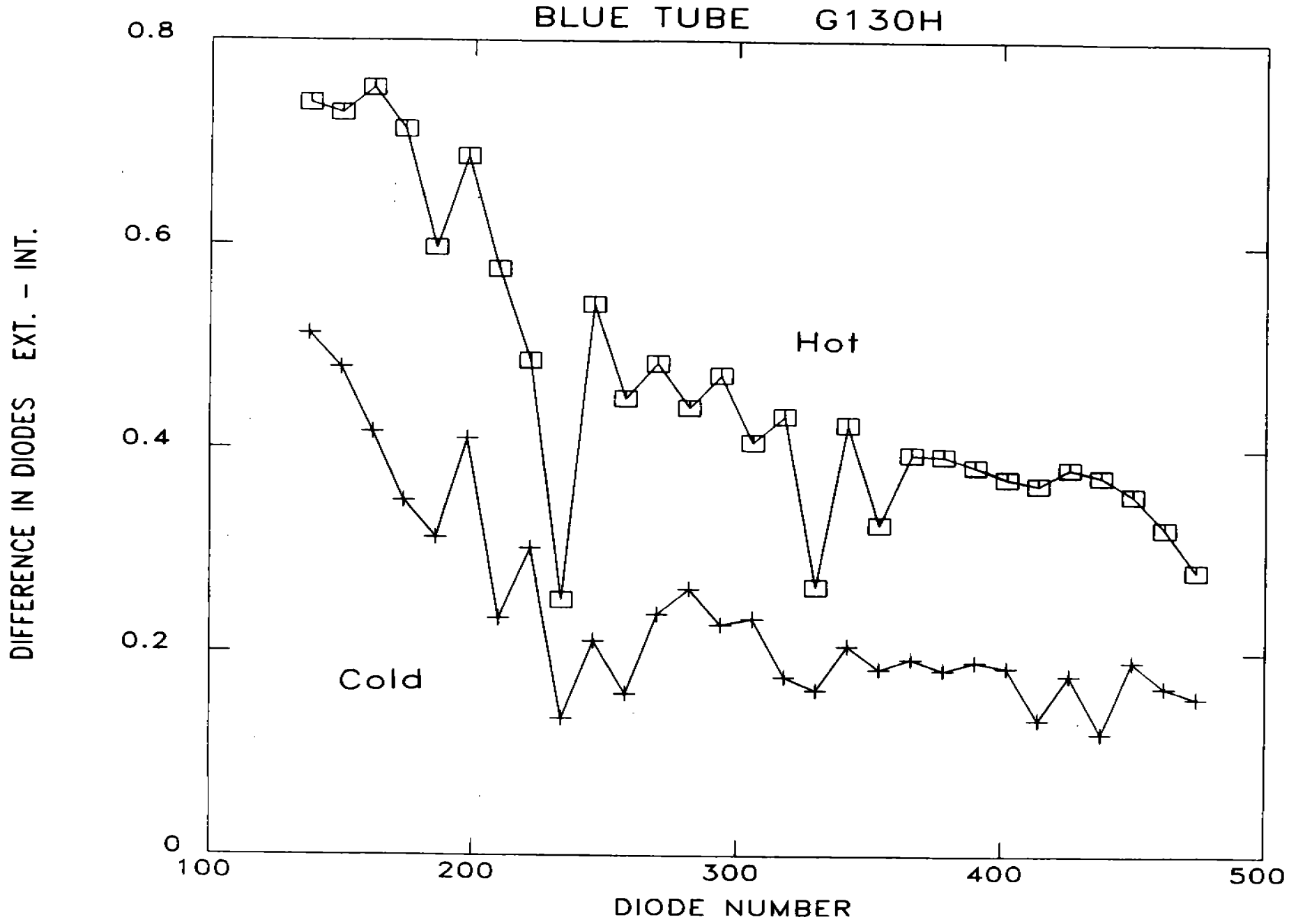
BLUE TUBE G130H
DIFFERENCE IN DIODES EXT. - INT.
0.8
0.6
0.4
0.2
0
Hot
Cold
100
200
300
400
500
DIODE NUMBER

Figure 10.